Spatiotemporal Patterns in Ultraslow Domain Wall Creep Dynamics

Ezequiel E. Ferrero,[1,*] Laura Foini,[2] Thierry Giamarchi,[2] Alejandro B. Kolton,[3] and Alberto Rosso[4]
[1]Université Grenoble Alpes, LIPHY, F-38000 Grenoble, France and CNRS, LIPHY, F-38000 Grenoble, France
[2]Department of Quantum Matter Physics, University of Geneva, 24 Quai Ernest-Ansermet, CH-1211 Geneva, Switzerland
[3]Instituto Balseiro-UNCu and CONICET, Centro Atómico Bariloche, 8400 Bariloche, Argentina
[4]LPTMS, CNRS, Université Paris-Sud, Université Paris-Saclay, 91405 Orsay, France
(Received 8 July 2016; published 7 April 2017)

In the presence of impurities, ferromagnetic and ferroelectric domain walls slide only above a finite external field. Close to this depinning threshold, they proceed by large and abrupt jumps called avalanches, while, at much smaller fields, these interfaces creep by thermal activation. In this Letter, we develop a novel numerical technique that captures the ultraslow creep regime over huge time scales. We point out the existence of activated events that involve collective reorganizations similar to avalanches, but, at variance with them, display correlated spatiotemporal patterns that resemble the complex sequence of aftershocks observed after a large earthquake. Remarkably, we show that events assemble in independent clusters that display at large scales the same statistics as critical depinning avalanches. We foresee these correlated dynamics being experimentally accessible by magnetooptical imaging of ferromagnetic films.

DOI: 10.1103/PhysRevLett.118.147208

The physics of disordered elastic systems is relevant for many areas of physics such as magnetic [1–5] and ferroelectric [6,7] domain wall, contact lines in wetting [8], crack propagation [9,10], and vortex lines in type-II superconductors [11]. It involves the driven motion of an elastic object, such as a manifold or a periodic structure, in a weakly disordered medium. At zero temperature, setting the system in motion requires the application of a finite force f exceeding a critical value f_c, a process known as depinning. When $f \gg f_c$, and due to dissipation, the system flows with a velocity essentially proportional to the driving force f, while it is pinned for $f < f_c$. At a finite temperature, this behavior is drastically modified since energy barriers can always be passed by thermal activation, leading to a finite velocity for any finite force.

One of the important questions is the response of an elastic interface to a very small force, $f \ll f_c$. Understanding this regime is relevant to assess the electrical resistance of a superconductor [11] or to judge in which conditions ferroelectric or ferromagnetic materials can be used to store and retrieve information [12]. It is now well known that at very low driving, the response is highly nonlinear, leading to the so-called *creep regime*. Phenomenological arguments based on the Arrhenius activation of segments of the interface (thermal nuclei) showed that, instead of a linear response, one should expect a stretched exponential response [13–17], where the average velocity of the wall is exponentially small in a power law of the external force. This behavior was later confirmed by more microscopic derivations based on a functional renormalization group procedure (FRG) in $d = 4 - \epsilon$ dimensions [18,19]. Experiments on magnetic and ferroelectric domain walls also provided confirmation of the creep law for the average velocity [1,6].

Despite these important successes between experiments and FRG, two important questions remain open concerning the creep motion. (i) First, a convincing confirmation of the creep law is still missing. While experiments typically concern systems in $d = 1$ and $d = 2$, the FRG is valid only in $d = 4 - \epsilon$, with ϵ assumed to be small. The only available theoretical tools to address the dynamics of low dimensional interfaces, so far, are numerical simulations. In this respect, traditional molecular dynamics techniques have difficulties reaching the very long times which are necessary to deal with the ultraslow motion characterizing creep [17,20]. Thus, a well-controlled numerical technique that would not suffer from slowing down when the force is reduced would be highly suitable. (ii) Second, and more importantly, the understanding of creep dynamics besides its mean velocity is an open issue. The FRG suggests that beyond the size of the thermal nucleus, the coarse-grained motion should be depinning-like up to a second temperature-controlled and very large length scale where the flow regime occurs [18,19]. However, the evidence of such a large scale and the description of this depinning-like motion are still elusive.

In this Letter, we provide a novel numerical technique able to tackle the creep at very small forces and vanishing temperature, computing the full sequence of activated events. We determine the distribution of their sizes—which displays an anomalous power-law behavior—and study their surprising spatiotemporal organization: initial seeds trigger large reorganizations of events (as shown in Fig. 1), statistically identical at large scales to deterministic depinning avalanches. In this way, our results give a clear interpretation of the FRG predictions. Further, they link the creep motion with the complex earthquake dynamics

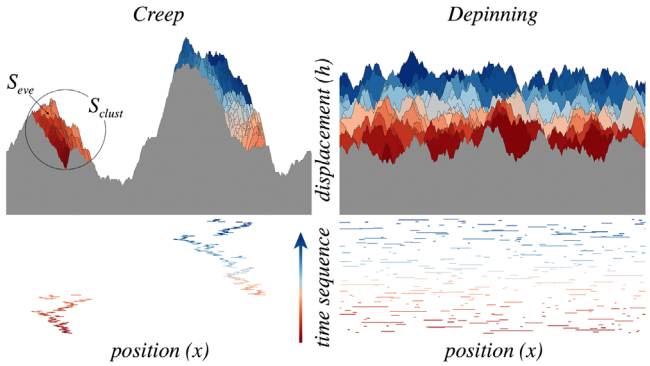

FIG. 1. Spatiotemporal patterns. Top: snapshot of 300 consecutive configurations for the moving interface. On the left, a typical sequence of events at a small force in the creep regime that assemble in space on a pattern of two clusters. On the right, a typical sequence of deterministic avalanches at a larger force close to depinning that appear randomly distributed in space. Bottom: activity maps showing for each event of the top row, a horizontal line representing its lateral extension. In all cases, the time sequence is illustrated by a color code, from dark red (older) to dark blue (more recent).

[21], where a main shock triggers a cascade of aftershocks [21–24]. We foresee these correlated dynamics being experimentally accessible by events' detection in ferromagnetic films [4]. To motivate such an experimental test, we specify the relevant scales for the particular case of Pt/Co/Pt films [25].

Phenomenology.—We consider a $d=1$-dimensional interface in absence of overhangs. At any time t, the local displacement is described by a single valued function, $h(x,t)$, which, in the overdamped limit, is described by the so-called quenched Edwards-Wilkinson equation [26–28]:

$$\gamma\partial_t h(x,t) = c\nabla^2 h(x,t) + f + F_p(x,h) + \eta(x,t), \quad (1)$$

where $c\nabla^2 h(x,t)$ accounts for the elastic force due to the surface tension, f is the external pulling force, and the fluctuations induced by impurities and temperature are encoded in the quenched disorder term $F_p(x,h)$ and in the Langevin thermal noise $\eta(x,t)$, respectively. We consider here random bond (RB) disorder in which the pinning potential is short-range correlated in the direction of motion. The analysis of the random-field disorder case, where the pinning force is short-range correlated (and thus, the energy displays correlations in the direction of motion), is deferred to the Supplemental Material [29].

At zero temperature, there are two reference points where self-affinity and scale-free behavior are expected.

Equilibrium scaling.—The first reference point, at $f=0$ corresponds to thermodynamic equilibrium where the extensive ground state energy displays a critical sample to sample fluctuations, growing as $L^{\theta_{eq}}$, and the interface is rough with a self-affine width growing as $L^{\zeta_{eq}}$. The exponents θ_{eq} and ζ_{eq} are universal and depend only on dimension, range of elastic interactions, and disorder class.

Depinning scaling.—The second critical point at $f=f_c$ and zero temperature corresponds to the depinning transition above which the interface acquires a finite global velocity $V \sim (f-f_c)^{\beta_{dep}}$. This point is characterized by a roughness ζ_{dep} (see Fig. 2 at $f=f_c$). At any force close to f_c, a small perturbation can induce a large reorganization of the interface, called depinning avalanche. The avalanche size, namely the area spanned by the moving interface, has power-law statistics with exponent [37,38]

$$\tau_{dep} = 2 - \frac{2}{d+\zeta_{dep}}. \quad (2)$$

Creep scaling.—At small but *finite* temperature ($T>0$) and below f_c, the instantaneous dynamics appears as a collection of incoherent vibrations localized around deep metastable configurations. However, the presence of a small positive drive makes a global forward motion energetically favorable in the long term. It was shown that at vanishing temperature, this forward motion is effectively dominated by the sequence of metastable states of decreasing energy, separated by the minimal energy barrier [39,40]. Scaling arguments suggest that at a very small force (i.e., in the creep regime), the *typical* size for these activated rearrangements is

$$L_{opt}(f) \sim 1/f^{\nu_{eq}}, \quad \text{with} \quad \nu_{eq} = \frac{1}{d+\zeta_{eq}-\theta_{eq}}. \quad (3)$$

The global velocity is determined using the Arrhenius formula, assuming that the energy barriers scale as the ground state fluctuations, i.e., as L_{opt}^{θ} with $\theta=\theta_{eq}$, resulting in the creep law [13–19]

$$-\log V \propto f^{-\mu}, \quad (4)$$

where $\mu = \nu_{eq}\theta_{eq} = \theta_{eq}/(d+\zeta_{eq}-\theta_{eq})$.

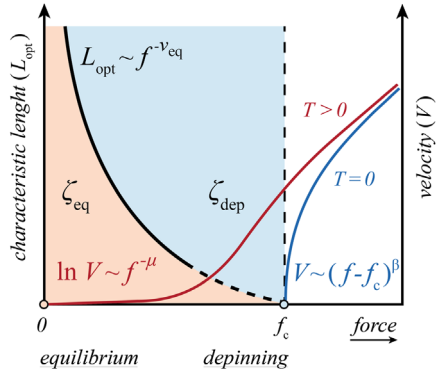

FIG. 2. Velocity-force characteristics and reference points. Two aspects of the $T>0$ dynamics below f_c are schematically shown: (i) the velocity V has a finite value at low forces well approximated by Eq. (4), and (ii) a characteristic length scale L_{opt}, which diverges as f goes to zero, separates two dynamical regimes identified by different roughness exponents, ζ_{eq} below L_{opt} and ζ_{dep} above L_{opt}. When $f \to f_c$, L_{opt} is identified with the microscopic Larkin length [16].

In order to overcome the difficulties of the traditional integration schemes for Eq. (1), it has been proposed to target the rare events that move the interface forward [39,40]. This corresponds to enumerate all pathways that end in a state with lower energy and select the one that has overcome the smallest barrier. Unfortunately, this exact enumeration grows exponentially with $L_{\rm opt}$ and does not permit to access the creep regime and to test the scaling arguments of Eqs. (3) and (4).

Modeling.—Below f_c, the dynamics that evolves the interface from one metastable state to the next one is composed by two steps: an *activated move* to jump a barrier and find a lower energy state, followed by a *deterministic relaxation* that further drives the interface through the energy lowering gradient until the next minimum is reached. The difference between the new and the previous metastable configurations is a compact object that we call an *event*, well characterized both by its area $S_{\rm eve}$ and by its lateral size $L_{\rm eve}$.

In order to explore the low force regime, we adopt here a new strategy for the activated move. Thanks to the Dijkstra algorithm, we compute (in a polynomial time) the minimal rearrangement *in size* that takes the interface to a lower energy state. At small forces, this approximate method is equivalent to searching for a minimal barrier since they grow with the size of the rearrangement. This strategy allows us to overcome the severe computation limitations of the exact algorithm and make it possible not only to increase by a factor 30 the system size, but, and more importantly, to decrease by a factor 100, the external drive f. Numerical checks show that even at forces smaller and comparable to f_c, the approximated method provides the same macroscopic dynamics as the exact algorithm. We refer the reader to the Supplemental Material [29] for this validation and algorithmic details. For a given realization of the disorder, the sequence of metastable configurations generated by our algorithm is unique once the steady state is reached. A typical sequence of locked configurations can be seen in Fig. 1 (left). Unless specified, all the reported numerical data correspond to a system size $L = 3360$.

Results analysis.—From the conventional picture of creep dynamics, one would expect that for small driving forces ($f \ll f_c$), the event size fluctuates around a "typical" value $L_{\rm opt}^{d+\zeta_{\rm eq}}$ (note that when $f \ll f_c$, the rearrangements induced by relaxation are minimal). However, in Fig. 3, we show that the event size distribution displays an unexpected power-law scaling:

$$P(S_{\rm eve}) \sim S_{\rm eve}^{-\tau} G(S_{\rm eve}/S_c), \tag{5}$$

similar to the depinning one with a force-dependent cutoff $S_c(f)$. A good collapse of the distributions at different forces is found for $S_c(f) \sim f^{-\alpha}$, with $\alpha = 1.25$. This scaling with force is perfectly consistent with the cutoff being $S_c \simeq S_{\rm opt} \sim L_{\rm opt}^{d+\zeta_{\rm eq}}$; that for $d = 1$ yields $\alpha = (1+\zeta_{\rm eq})\nu_{\rm eq} = 5/4$. We conclude that at variance with standard scaling, the

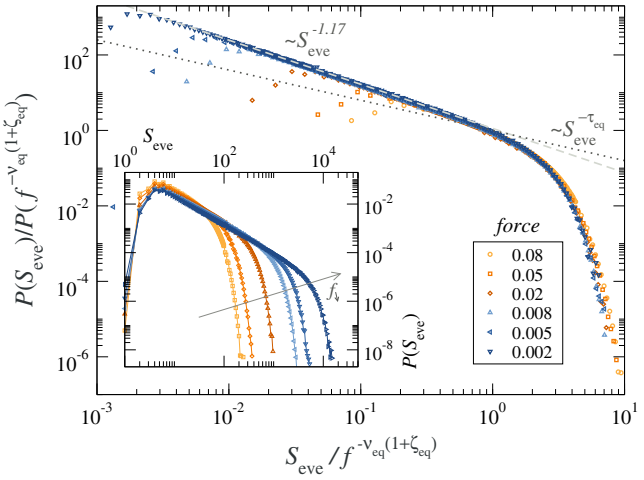

FIG. 3. Events' size distributions $P(S_{\rm eve})$ at different forces (inset), collapsed by plotting $P(S_{\rm eve})/P(S_c)$ vs $S_{\rm eve}/S_c$, with $S_c(f) = f^{-\nu_{\rm eq}(1+\zeta_{\rm eq})}$ (main panel), therefore validating the expected creep scaling $L_{\rm opt} \sim f^{-\nu_{\rm eq}}$, given $S_c \sim L_{\rm opt}^{(1+\zeta_{\rm eq})}$.

characteristic length $L_{\rm opt}$ corresponds to the "largest" rather than the "typical" size of the irreversible events. However, the creep law (4) is not affected, since, for activated dynamics, the velocity is controlled by the largest barriers and therefore by $L_{\rm opt}$. Notice that for larger forces ($f \to f_c^-$), the activated nucleus $L_{\rm opt}$ saturates to a microsopic length, but the event size is dominated by the deterministic relaxation [40] so that $L_{\rm eve}$ diverges as $(f_c - f)^{-\nu_{\rm dep}}$. Therefore, also $S_{\rm eve}$ (defined as combination of an activated and a deterministic move) diverges at both critical points while taking a minimal value at intermediate forces (see Supplemental Material [29]).

A second important feature of $P(S_{\rm eve})$ is the power-law decay. A scaling argument, valid for elastic systems [41], suggests that the cutoff exponent α and the power-law exponent τ should satisfy the relation $\tau = 2 - 2\nu_{\rm eq}/\alpha = 2 - 2/(d+\zeta_{\rm eq})$, in analogy to Eq. (2). Here, the cutoff $\sim f^{-\alpha}$ is controlled by the distance to equilibrium $f = 0$, and we would expect the value $\tau = \tau_{\rm eq} = 4/5$. However, this is not the case, and we find a larger exponent $\tau = 1.17 \pm 0.01$. Such a distribution with $\tau > \tau_{\rm eq}$, violating the scaling relation, expresses an excess of small events compared to what is expected *a priori* for a distribution of fully independent avalanches.

To shed light on this issue, we further inspect Fig. 1. We observe that creep events are organized in compact spatio-temporal patterns in contrast with depinning avalanches that appear randomly distributed along the interface, as well illustrated by the *activity maps* that supplement the sequence of metastable configurations. Remarkably, there is a similarity of such time correlations between events with the ones observed in real earthquakes, where a large main shock is followed by a cascade of aftershocks [21–24]. The statistics of the energy dissipated by earthquakes is characterized by the Gutenberg-Richter exponent b, which is equivalent to the

exponent τ via the exact relation $b = \frac{3}{2}(\tau - 1)$. For classic avalanche models (e.g., depinning, directed percolation, Abelian sandpiles), the maximal value for b is $3/4$ (which corresponds to the mean field exponent $\tau = 3/2$). From the analysis of the seismic records, one gets [21,22] $b \simeq 1 > 3/4$. Thus, we observe that, due to the presence of time correlation in the sequence of events, both earthquakes and creep events display an effective exponent τ bigger than the one predicted by simple avalanche models.

In the interest of evaluating these spatiotemporal patterns, we collect correlated events in *clusters* (creep events enclosed by a circle in Fig. 1). In presence of short range elasticity, a simple criterion for the cluster formation is to add a new event to a growing cluster if their spatial overlap is not null. The growth of a cluster stops whenever a new event has no overlap with it. This event, in turn, represents the seed for the creation of a new cluster. In finite systems, this procedure can generate system sized clusters, and in this case, we decide to artificially break the cluster construction and start with a new cluster. This finite-size effect is mitigated here by considering big enough systems, its analysis being the goal of a separate work [42]. Upon identifying the sequence of clusters, one can compute their size, namely the sum of the areas of all the events that compose the cluster.

Figure 4 shows the cluster size distribution $P(S_{\rm clust})$ that displays a crossover at a value $S_{\rm clust} \simeq S_{\rm opt}$. Below $S_{\rm opt}$, we observe a power law with exponent $\approx 0.80 \pm 0.06$, consistent with the equilibrium value, $\tau_{\rm eq} = \frac{4}{5}$. Above $S_{\rm opt}$, instead, the power-law exponent $\approx 1.11 \pm 0.04$ is in good agreement with the depinning critical avalanches distribution value [38] $\tau_{\rm dep} \sim 1.11$. In order to span more than eight decades in $S_{\rm clust}/S_{\rm opt}$, we have simulated a range of forces $f \in \{0.002, 0.2\}$. The equilibrium exponent appears in the limit of small forces, while forces larger than $f \simeq 0.05$ only display the depinning exponent $\tau_{\rm dep}$, with a lower cutoff around $S_{\rm opt}$. The upper cutoff of the distribution is controlled by the system size and diverges in the thermodynamic limit.

The inset of Fig. 4 shows the structure factor $S(q)$ $S(q) = \overline{h_q h_{-q}}$ (here, h_q is the Fourier transform of a metastable configuration $h(x)$ in the steady state, and the overline stands for the average over many metastable configurations). The figure clearly shows a crossover length scale $1/q_c \sim L_{\rm opt} \sim f^{-\nu_{\rm eq}}$ that separates short scales (large q) displaying an equilibrium roughness exponent $\zeta_{\rm eq} = 2/3$ from large scales (small q) displaying a depinning roughness $\zeta_{\rm dep} \approx 1.25$, in agreement with Refs. [43] and [44,45], respectively. This geometrical crossover is compatible with the exponent crossover in the clusters' size distribution and supports the idea of these objects being depinning-like above a scale $L_{\rm opt}$. The robustness of this conclusion is confirmed by the study of the random field (RF) disorder case, which belongs to a different universality class at equilibrium but shares the same exponents as RB at the depinning transition [19,37,45] (see Supplemental Material [29]).

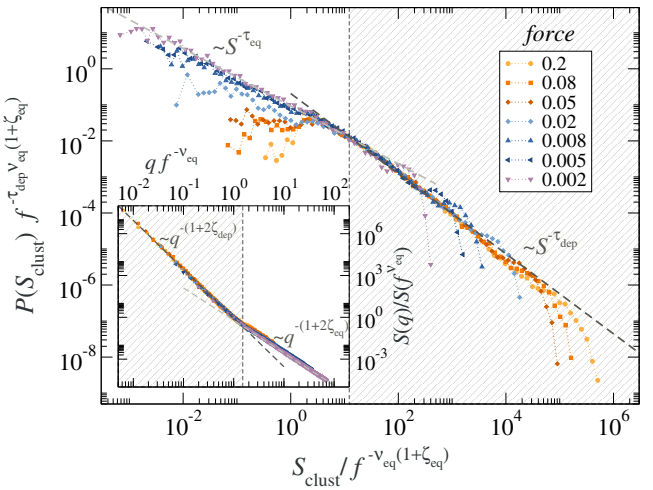

FIG. 4. Cluster area distribution $P(S_{\rm clust})$ for different forces $f \in \{0.002, 0.2\}$. A characteristic size $S_{\rm opt} \sim S_c \simeq L_{\rm opt}^{(1+\zeta_{\rm eq})}$, with $L_{\rm opt} \sim f^{-\nu_{\rm eq}}$, separates small clusters that follow equilibriumlike statistics from big clusters that follow a depinning-like one (shaded range). Inset: rescaled structure factor $S(q)$ for the same forces. $S(q)/S(q_c)$ is a function of q/q_c, with $q_c \sim 1/L_{\rm opt} \sim f^{\nu_{\rm eq}}$, denoting a geometrical crossover from an equilibriumlike roughness at small scales to a depinning-like roughness at large scales.

Discussion.—Our newly developed algorithm allows us to go deep in the creep regime of an elastic interface moving in a disordered environment. It gives us an accurate description of the forward irreversible motion in terms of a sequence of well-defined activated events that goes far beyond the FRG analysis. The most striking property emerging from our study of creep events is their occurrence in correlated spatiotemporal patterns, in sharp contrast with depinning avalanches nucleating randomly along the line. Despite the novel properties displayed by such dynamics, we find that the creep law is verified by measuring below $f = 0.1$ a divergence compatible with $L_{\rm opt} \sim f^{-\nu_{\rm eq}}$ and therefore, with Eq. (4).

We have constructed collective avalanches or "clusters" of creep events. We identify their sequence with the depinning-like motion predicted by the FRG analysis [19] at intermediate scales above $L_{\rm opt}$ and below a temperature-dependent length (denominated $L_{\rm av}$), which diverges for $T \to 0$. Because of the imposed limit of vanishing temperature in our study, the cluster statistics are scale free; otherwise, we would expect a cutoff related to $L_{\rm av}$. Remarkably, we find out that the dynamics inside the cluster is *activated*, as creep events are required to overcome energy barriers, and not simply a *deterministic* gradient-descent motion. Not being fully anticipated by FRG, our picture opens a door for future theoretical studies.

We believe that the clustering behavior of creep events can be observed in experiments with the current magnetooptical techniques able to directly visualize the interface motion. In fact, monitoring ion-irradiated magnetic thin films,

Repain *et al.* [4] were able to observe small correlated events in the creep regime, their characteristic size increasing when lowering the external field, in good qualitative agreement with our predictions. Furthermore, we can quantitatively anticipate the observation of spatially resolved individual creep events on Pt(0.35 nm)/Co(0.45 nm)/Pt(0.35 nm) films [25] at room temperature for domain wall velocities of order 1 nm/s (see Supplemental Material [29]). We expect not only direct visualizations but also noise measurements [46–48] to allow for a full quantitative test of our predictions on creep dynamics.

Despite the experimental interest, there are few theoretical studies on avalanches' dynamics at finite temperature. One should mention the Bak-Sneppen model of biological evolution, where the successful mutations are activated over finite barriers [49] and induce scale free patterns of spatially correlated mutations similar to our clusters.

E. E. F acknowledges financial support from ERC Grant No. ADG20110209. This work was supported in part by the Swiss SNF under Division II. A. B. K. acknowledges partial support from Projects CONICET-PIP11220120100250CO and ANPCyT-PICT-2011-1537 (Argentina). Most of the computations were performed using the Froggy platform of the CIMENT infrastructure supported by the Rhône-Alpes region (Grant No. CPER07-13 CIRA) and the Equip@Meso Project (Reference No. ANR-10-EQPX-29-01). We thank M. V. Duprez for her help on the schematic figures. We especially thank E. A. Jagla for driving our attention to the spatiotemporal patterns in the Bak-Sneppen model. Further, we would like to express our gratitude to S. Bustingorry, J. Curiale, M. Granada, V. Jeudy, V. Lecomte, and A. Mougin for fruitful discussions.

*Present address: Department of Physics, University of Milano, via Celoria 16, 20133 Milano, Italy.
ezequiel.ferrero@unimi.it

[1] S. Lemerle, J. Ferré, C. Chappert, V. Mathet, T. Giamarchi, and P. Le Doussal, Phys. Rev. Lett. **80**, 849 (1998).
[2] M. Yamanouchi, D. Chiba, F. Matsukura, T. Dietl, and H. Ohno, Phys. Rev. Lett. **96**, 096601 (2006).
[3] P. J. Metaxas, J. P. Jamet, A. Mougin, M. Cormier, J. Ferré, V. Baltz, B. Rodmacq, B. Dieny, and R. L. Stamps, Phys. Rev. Lett. **99**, 217208 (2007).
[4] V. Repain, M. Bauer, J.-P. Jamet, J. Ferré, A. Mougin, C. Chappert, and H. Bernas, Europhys. Lett. **68**, 460 (2004).
[5] V. Jeudy, A. Mougin, S. Bustingorry, W. S. Torres, J. Gorchon, A. B. Kolton, A. Lemaître, and J.-P. Jamet, Phys. Rev. Lett. **117**, 057201 (2016).
[6] T. Tybell, P. Paruch, T. Giamarchi, and J.-M. Triscone, Phys. Rev. Lett. **89**, 097601 (2002).
[7] P. Paruch and J.-M. Triscone, Appl. Phys. Lett. **88**, 162907 (2006).
[8] S. Moulinet, C. Guthmann, and E. Rolley, Eur. Phys. J. E **8**, 437 (2002).
[9] E. Bouchaud, J. Bouchaud, D. Fisher, S. Ramanathan, and J. Rice, J. Mech. Phys. Solids **50**, 1703 (2002).
[10] S. Zapperi, M. Alava, and P. Nukala, Adv. Phys. **55**, 349 (2006).
[11] G. Blatter, M. Feigel'Man, V. Geshkenbein, A. Larkin, and V. M. Vinokur, Rev. Mod. Phys. **66**, 1125 (1994).
[12] S. S. Parkin, M. Hayashi, and L. Thomas, Science **320**, 190 (2008).
[13] L. Ioffe and V. Vinokur, J. Phys. C **20**, 6149 (1987).
[14] T. Nattermann, Europhys. Lett. **4**, 1241 (1987).
[15] M. V. Feigel'man, V. B. Geshkenbein, A. I. Larkin, and V. M. Vinokur, Phys. Rev. Lett. **63**, 2303 (1989).
[16] T. Nattermann, Y. Shapir, and I. Vilfan, Phys. Rev. B **42**, 8577 (1990).
[17] M. Dong, M. C. Marchetti, A. A. Middleton, and V. Vinokur, Phys. Rev. Lett. **70**, 662 (1993).
[18] P. Chauve, T. Giamarchi, and P. Le Doussal, Europhys. Lett. **44**, 110 (1998).
[19] P. Chauve, T. Giamarchi, and P. Le Doussal, Phys. Rev. B **62**, 6241 (2000).
[20] A. B. Kolton, A. Rosso, and T. Giamarchi, Phys. Rev. Lett. **94**, 047002 (2005).
[21] C. H. Scholz, *The Mechanics of Earthquakes and Faulting* (Cambridge University Press, New York, 2002).
[22] E. A. Jagla, F. P. Landes, and A. Rosso, Phys. Rev. Lett. **112**, 174301 (2014).
[23] E. A. Jagla and A. B. Kolton, J. Geophys. Res. **115**, B05312 (2010).
[24] L. de Arcangelis, C. Godano, J. R. Grasso, and E. Lippiello, Phys. Rep. **628**, 1 (2016).
[25] J. Gorchon, S. Bustingorry, J. Ferré, V. Jeudy, A. B. Kolton, and T. Giamarchi, Phys. Rev. Lett. **113**, 027205 (2014).
[26] D. S. Fisher, Phys. Rep. **301**, 113 (1998).
[27] M. Kardar, Phys. Rep. **301**, 85 (1998).
[28] E. E. Ferrero, S. Bustingorry, A. B. Kolton, and A. Rosso, C.R. Phys. **14**, 641 (2013).
[29] See Supplemental Material http://link.aps.org/supplemental/10.1103/PhysRevLett.118.147208, which includes Refs. [43–49], for model details and validation, random field disorder case and quantitative estimates for Pt/Co/Pt thin films.
[30] A. Rosso and W. Krauth, Phys. Rev. B **65**, 012202 (2001).
[31] A. Rosso and W. Krauth, in *Proceedings of the Europhysics Conference on Computational Physics, 2004*, edited by M. Ferrario, S. Melchionna, and C. Pierleoni [Comput. Phys. Commun. **169**, 188 (2005)].
[32] D. S. Fisher, Phys. Rev. Lett. **56**, 1964 (1986).
[33] P. Chauve, P. Le Doussal, and K. Wiese, Phys. Rev. Lett. **86**, 1785 (2001).
[34] A. Larkin and Y. N. Ovchinnikov, J. Low Temp. Phys. **34**, 409 (1979).
[35] V. Démery, A. Rosso, and L. Ponson, Europhys. Lett. **105**, 34003 (2014).
[36] K.-J. Kim, J.-C. Lee, S.-M. Ahn, K.-S. Lee, C.-W. Lee, Y. J. Cho, S. Seo, K.-H. Shin, S.-B. Choe, and H.-W. Lee, Nature (London) **458**, 740 (2009).
[37] O. Narayan and D. S. Fisher, Phys. Rev. B **48**, 7030 (1993).
[38] A. Rosso, P. Le Doussal, and K. J. Wiese, Phys. Rev. B **80**, 144204 (2009).

[39] A. B. Kolton, A. Rosso, T. Giamarchi, and W. Krauth, Phys. Rev. Lett. **97**, 057001 (2006).
[40] A. B. Kolton, A. Rosso, T. Giamarchi, and W. Krauth, Phys. Rev. B **79**, 184207 (2009).
[41] P. Le Doussal, A. A. Middleton, and K. J. Wiese, Phys. Rev. E **79**, 050101 (2009).
[42] E. Ferrero, L. Foini, T. Giamarchi, A. Kolton, and A. Rosso (to be published).
[43] M. Kardar, Phys. Rev. Lett. **55**, 2923 (1985).
[44] A. Rosso, A. K. Hartmann, and W. Krauth, Phys. Rev. E **67**, 021602 (2003).
[45] E. E. Ferrero, S. Bustingorry, and A. B. Kolton, Phys. Rev. E **87**, 032122 (2013).
[46] S. Zapperi, P. Cizeau, G. Durin, and H. E. Stanley, Phys. Rev. B **58**, 6353 (1998).
[47] G. Durin and S. Zapperi, Phys. Rev. Lett. **84**, 4705 (2000).
[48] G. Durin, F. Bohn, M. A. Correa, R. L. Sommer, P. Le Doussal, and K. J. Wiese, Phys. Rev. Lett. **117**, 087201 (2016).
[49] P. Bak and K. Sneppen, Phys. Rev. Lett. **71**, 4083 (1993).